Adaptive Vibration Control for an Active Mass Damper of a High-rise Building

Jiali Feng and Zhijie Liu* and Xiuyu He and Qiang Fu and Guang Li

***Abstract*—As a kind of large flexible structure, high-rise buildings need to consider wind-resistant and anti-seismic problems for the safety of occupants and properties, especially in coastal areas. This paper proposes an infinite dimensional model and an adaptive boundary control law for an active mass damper(AMD) on this question. The dynamic model of the high-rise building is a combination of some storeys which have flexible walls and rigid floors under a series of physical conditions. Then the adaptive boundary controller is acted on an AMD which is equipped on the top floor, in order to suppress the vibration of every floor and guarantee the comfort of residents. Moreover, simulations and experiments are carried out on a two-floor flexible building to illustrate the effectiveness of the proposed control strategy.**

***Index Terms*—Adaptive Control, Vibration Control, Active Mass Damper(AMD), Distributed Parameter System, High-rise Buildings.**

I. Introduction

To guarantee the occupant comfort, high-rise buildings need to satisfy some standards, for example the ISO Building Standards ISO 9882-1993 and ISO 9883-1993, the National Standard of P. R. China JGJ3-2002 where the maximum accelerate of public buildings is requested less than 0.28m/s^2, and the National Standard of P. R. China JGJ99-98 where the maximum accelerate of apartment buildings is required less than 0.20m/s^2. These standards require high-rise buildings to increase the damp of structures and to suppress vibrations induced by typhoons or earthquakes [1]. Many high-rise buildings have considered this problem in engineering. The One Wall Centre in Vancouver (157.8m) installs tuned liquid column dampers to guarantee the comfort of the building. The Taipei 101 Tower in Taipei (509.2m) [2] and the Canton Tower in Guangzhou (454m) [3] use semi-active and active tuned mass dampers for vibration suppression, respectively.

On the basis of various vibration suppression systems, many studies are proposed in passive, semi-active, active, and hybrid control design to suppress the vibration. The development of vibration control of building and bridge structures since 2013 is introduced in [4], and above four kinds of control methods are analyzed in detail. Passive control methods can increase the damp of structures and modify the stiffness of structures. However passive control cannot adapt well to changeful natural frequency caused by structural nonlinearities and huge seismic excitations, especially for multiple floor buildings [5]. Thus, researchers have been paying more attention to active, semi-active and hybrid control methods recently [6], [7]. A review of control algorithms and optimal methods for active or semi-active devices before 2015 is presented in [8].

To combine the advantages of active control algorithms and vibration suppression devices in high-rise buildings, such as AMDs and active tendons, many researchers have proposed some control methods applied on these systems. The authors in [9] propose a tuned mass damper and use H_2 linear quadratic Gaussian control algorithm to design a kind of vibration suppression precesses. A filtered sliding mode control method is used for suppressing the vibration of a 76-storey building with an active tuned mass damper in [10]. In [11], on the basis of a modified Newton's method, a multilayer feedforward neural network is presented for suppressing the vibration of a four-storey building structure. In [12], a multi-objective adaptive genetic-fuzzy control strategy is used on an AMD to reduce the wind-induced vibration.

Although many researchers have already proposed some solutions for solving the wind-resistant and anti-seismic problems, the accuracy of the models of the high-rise buildings with vibration suppression devices needs further improvement. The models of flexible building structures are mainly considered as first order or second order finite dimensional models. For example, the authors in [9] use the Lagrangian method to establish the model which is described by ordinary differential equations. However, because of the flexibility of high-rise buildings, they really belong to distributed parameter systems and should be described by partial differential equations [13], [14], [15], [16]. Further, considering that high-rise buildings are slender with a relatively large height-to-width ratio, they can be modeled as Euler-Bernoulli beams [17], [18], [19] which have been used in various systems. Comparing with the Euler-Bernoulli beam model used in flexible robot arms [20], [21], flexible satellites [22], [23] and marine risers [24], [25], the model in this paper has different physical conditions: the top and bottom ends of the different flexible walls in every storey are connected by rigid floors respectively.

Bestowed upon a partial differential equation model, both boundary control [26], [27] and distributed control can enable

This work is supported by National Natural Science Foundation of China under Grant 62073030 the Interdisciplinary Research Project for Young Teachers of USTB under Grant FRF-IDRY-19-024, the Fundamental Research Funds for the China Central Universities of USTB under Grant FRF-TP-19-001B2, Postdoctor Research Foundation of Shunde Graduate School of University of Science and Technology Beijing under Grant 2020BH002Scientific and Technological Innovation Foundation of Shunde Graduate School, USTB under Grant BK19BE015and Beijing Top Discipline for Artificial Intelligent Science and Engineering, University of Science and Technology Beijing.

J. Feng and Z. Liu and X. He and Q. Fu are with Key Laboratory of Knowledge Automation for Industrial Processes of Ministry of Education, School of Automation and Electrical Engineering, and Institute of Artificial Intelligence, University of Science and Technology Beijing, Beijing 100083, China. (e-mail: liuzhijie2012@gmail.com)

G. Li is with School of Engineering and Materials Science, Queen Mary University of London, Mile End Road, London E1 4Ns, UK.

the control objectives of different distributed parameter systems to be achieved [28]. Many control method, like iterative learning control [29], [30], neural control [31], [32], and fuzzy control [33], can be designed as a boundary control strategy. Boundary control, as a control method that can be easily applied in practice [34], [35], is used to solve the problem in this paper. The authors in [36] design an output feedback boundary controller and an infinite-dimensional observer for a servo system to track a one-dimensional heat equation and resist external disturbance. In [37] and [38], using hyperbolic barrier Lyapunov functions, boundary control is proposed to a flexible string and a flexible satellite system, respectively. The authors in [39] apply two boundary controllers on a plant for grasping objectives. The plant is composed of two motors and two flexible robot arms, where the motors move on a slider in one dimension. Comparing with previous systems which always use different boundary controllers to control different Euler-Bernoulli beams or strings, this paper uses one actuator to control several beams simultaneously, which increases the challenge of the problem considered in this paper. Besides, considering that the physical parameters, like bending stiffness and tension of the walls, are difficult to measure, an adaptive controller would be needed in this problem [40], [41]. The authors in [42] use a robust adaptive boundary control method to suppress the transverse vibration of a axially moving string system, and use two adaptive laws to update the estimated values of the system parameters. By designing suitable adaptive laws, this paper is going to provide proper estimated values of the unknown physical parameters.

In general, the contributions of this paper can be summarised as follows. 1) Four Euler-Bernoulli beams, which are described by partial differential equations, are used to model a two-floor building structure with an AMD system, and an adaptive boundary control law is proposed to suppress the vibration of the building. Meanwhile, the closed-loop system can realize the asymptotically stability in theory. 2) The adaptive boundary control law in this paper is just applied on a cart moving on the top floor to suppress the vibration of the four beams. On the contrary, the pervious studies always use several controllers to control several beams, like [39]. 3) Experiments on the Quanser's building platform are implemented to verify the effectiveness of the proposed boundary control law.

In the rest of the paper, Section II describes the dynamic model of the building system. Section III proposes a boundary control law and discusses the stability of the closed-loop system. Section IV and Section V illustrate the accuracy of the dynamic model and the effectiveness of the boundary control law by carrying out some simulations and experiments. Finally, Section VI gives a brief conclusion of this paper.

II. Problem Formulation

The model in this paper mainly is bestowed upon the Quanser's building plant (Fig. 1) that is a two-storey flexible building-like structure on top of which a linear cart is driven by a rack and pinion mechanism.

The structure frame is made up of four flexible steel sheets and two rigid floors. Hence, four Euler-Bernoulli beams with some boundary conditions could describe the system (Fig. 2). H_f is the hight of one storey. M_f and M_c are the mass of a floor and the mass damper, respectively. $w_{1l}(y,t)$, $w_{1r}(y,t)$, $w_{2l}(y,t)$ and $w_{2r}(y,t)$ are elastic deflections of the left and right walls in the first and second storeys at the position y for time t, respectively. $w_{1l}(H_f,t)$ and $w_{1r}(H_f,t)$ are elastic deflections of the left and right walls at the top end. $w_{2l}(H_f,t)$ and $w_{2r}(H_f,t)$ are elastic deflections of the left and right walls at the bottom end. Because the top ends of the walls of the first storey and the bottom ends of the walls of the second storey are connected by first rigid floor, the vibrations at the four position are equal, namely, $w_{1l}(H_f,t) = w_{1r}(H_f,t) = w_{2l}(H_f,t) = w_{2r}(H_f,t) = w(H_f,t)$. Similarly, the vibrations at the top ends of the walls of the second storey are equal, namely, $w_{2l}(2H_f,t) = w_{2r}(2H_f,t) = w(2H_f,t)$. The mass damper moves in a straight line on the top of the floor and the initial position of the mass damper is on the center line the floor. The positive direction of the mass damper is same as the direction of X' axis. $x_c(t)$ is the mass damper's displacement in $X'O'Y'$ coordinates. $u(t)$ is the adaptive boundary control force. In addition, throughout the paper, we mark that $(\cdot)' = \partial(\cdot)/\partial y$, $(\cdot)'' = \partial^2(\cdot)/\partial y^2$, $(\cdot)''' = \partial^3(\cdot)/\partial y^3$, $(\cdot)'''' = \partial^4(\cdot)/\partial y^4$, $\dot{(\cdot)} = \partial(\cdot)/\partial t$ and $\ddot{(\cdot)} = \partial^2(\cdot)/\partial t^2$.

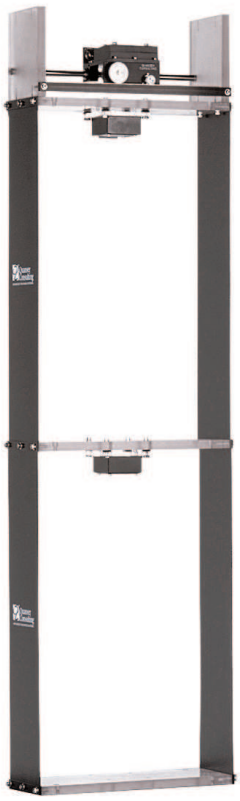

Fig. 1. The Quanser's building plant.

The kinetic energy of the building structure with the AMD $E_k(t)$ can be described as

$$E_k(t) = \frac{1}{2}\int_0^{H_f} \rho[\dot{w}_{1l}(y,t)]^2 dy + \frac{1}{2}\int_{H_f}^{2H_f} \rho[\dot{w}_{2l}(y,t)]^2 dy$$

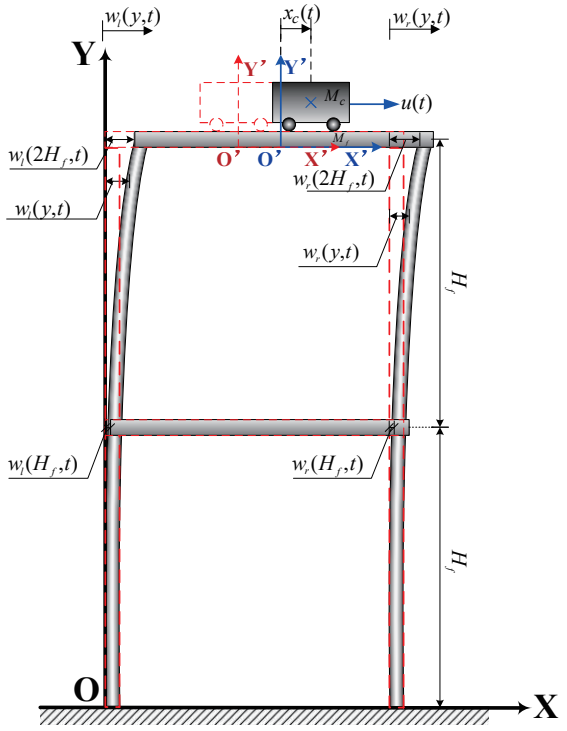

Fig. 2. The dynamic model of the building system.

$$
\begin{aligned}
&+\frac{1}{2}\int_0^{H_f}\rho[\dot{w}_{1r}(y,t)]^2dy+\frac{M_f}{2}[\dot{w}_1(H_f,t)]^2\\
&+\frac{1}{2}\int_{H_f}^{2H_f}\rho[\dot{w}_{2r}(y,t)]^2dy+\frac{M_f}{2}[\dot{w}_2(2H_f,t)]^2\\
&+\frac{M_c}{2}[\dot{x}_c(t)+\dot{w}_2(2H_f,t)]^2+\frac{J_c}{2}[\dot{x}_c(t)]^2 \qquad (1)
\end{aligned}
$$

where $\rho > 0$ is the uniform mass per unit length of a wall and four walls have same uniform density. J_c is the cart rotor moment of inertia. Then, considering that different walls have same bending stiffness and tension parameters, the potential energy of the building structure with the AMD $E_p(t)$ can be described as

$$
\begin{aligned}
E_p(t) \;=\; &\frac{1}{2}\int_0^{H_f}EI\{[w''_{1l}(y,t)]^2+[w''_{1r}(y,t)]^2\}dy\\
&+\frac{1}{2}\int_{H_f}^{2H_f}EI\{[w''_{2l}(y,t)]^2+[w''_{2r}(y,t)]^2\}dy\\
&+\frac{1}{2}\int_0^{H_f}T\{[w'_{1l}(y,t)]^2+[w'_{1r}(y,t)]^2\}dy\\
&+\frac{1}{2}\int_{H_f}^{2H_f}T\{[w'_{2l}(y,t)]^2+[w'_{2r}(y,t)]^2\}dy \qquad (2)
\end{aligned}
$$

where EI and T are bending stiffness and tension of a wall, respectively. Then, the virtual work $\delta W_{nc}(t)$ done by the non-conservative force can be represented as

$$
\delta W_{nc}(t) \;=\; u(t)\delta[x_c(t)+w_2(2H_f,t)]. \qquad (3)
$$

Using Hamilton's principle, we obtain motion equations of the building structure with the AMD as

$$
\begin{aligned}
&\rho\ddot{w}_{1l}(y,t)+EIw''''_{1l}(y,t)-Tw''_{1l}(y,t)=0 \qquad (4)\\
&\rho\ddot{w}_{1r}(y,t)+EIw''''_{1r}(y,t)-Tw''_{1r}(y,t)=0 \qquad (5)\\
&\qquad\qquad \forall(y,t)\in[0,H_f)\times[0,\infty)
\end{aligned}
$$

$$
\begin{aligned}
&\rho\ddot{w}_{2l}(y,t)+EIw''''_{2l}(y,t)-Tw''_{2l}(y,t)=0 \qquad (6)\\
&\rho\ddot{w}_{2r}(y,t)+EIw''''_{2r}(y,t)-Tw''_{2r}(y,t)=0 \qquad (7)\\
&\qquad\qquad \forall(y,t)\in[H_f,2H_f]\times[0,\infty)
\end{aligned}
$$

and boundary conditions as

$$
\begin{aligned}
&M_f\ddot{w}_2(2H_f,t)+T[w'_{2l}(2H_f,t)+w'_{2r}(2H_f,t)]\\
&-J_c\ddot{x}_c(t)-EI[w'''_{2l}(2H_f,t)+w'''_{2r}(2H_f,t)]=0 \qquad (8)\\
&M_f\ddot{w}_1(H_f,t)-EI[w'''_{1l}(H_f,t)+w'''_{1r}(H_f,t)\\
&-w'''_{2l}(H_f,t)-w'''_{2r}(H_f,t)]+T[w'_{1l}(H_f,t))\\
&+w'_{1r}(H_f,t-w'_{2l}(H_f,t)-w'_{2r}(H_f,t)]=0 \qquad (9)\\
&w_{1l}(0,t)=w_{1r}(0,t)=0 \qquad (10)\\
&w'_{1l}(0,t)=w'_{1r}(0,t)=0 \qquad (11)\\
&w''_{1l}(H_f,t)=w''_{1r}(H_f,t)=0 \qquad (12)\\
&w''_{2l}(H_f,t)=w'_{2r}(H_f,t)=0 \qquad (13)\\
&w''_{2l}(2H_f,t)=w''_{2r}(2H_f,t)=0 \qquad (14)\\
&M_c\ddot{w}_2(2H_f,t)+(M_c+J_c)\ddot{x}_c(t)=u(t) \qquad (15)\\
&\qquad\qquad \forall t\in[0,\infty)
\end{aligned}
$$

Remark 1. The equations (4)-(5) describe the dynamic characters of the left and right walls in the first storey, respectively. The equations (6)-(7) describe the dynamic characters of the left and right walls in the second storey, respectively. The boundary conditions (8) and (15) describe the connection between the top floor and the controller. The boundary condition (9) describes the connection between the first and second storeys. Other boundary conditions describe the dynamic characters of the first and second floors.

III. Control Design

This section presents the design of an exact model-based boundary controller and an adaptive boundary controller. In order to guarantee the occupant comfort within a short time when the buildings are in influenced by winds or earthquakes, the control objective is to suppress the vibration induced by the external disturbance.

A. Exact Model-Based Boundary Control

When all of the parameters in the model are measurable, an exact model-based boundary controller as follows can be designed to realize the control objectives, by using the

Lyapunov's direct method.

$$\begin{aligned}\mu(t) &= \dot{w}_2(2H_f,t) - \gamma_1[w'''_{2l}(2H_f,t) + w'''_{2r}(2H_f,t)] \\ &\quad +\gamma_2[w'_{2l}(2H_f,t) + w'_{2r}(2H_f,t)] \qquad (16)\\ u(t) &= -k\mu(t) + \Big(M_c + \frac{(M_c+J_c)M_f}{J_c}\Big)[\gamma_1\dot{w}'''_{2l}(2H_f,t) \\ &\quad +\gamma_1\dot{w}'''_{2r}(2H_f,t) - \gamma_2\dot{w}'_{2l}(2H_f,t) - \gamma_2\dot{w}'_{2r}(2H_f,t)] \\ &\quad -\frac{M_c+J_c}{J_c}EI[w'''_{2r}(2H_f,t) + w'''_{2l}(2H_f,t)] \\ &\quad +\frac{M_c+J_c}{J_c}T[w'_{2l}(2H_f,t) + w'_{2r}(2H_f,t)] \qquad (17)\end{aligned}$$

where γ_1, γ_2 and k are positive constants.

Consider the Lyapunov function candidate as

$$V(t) = V_a(t) + V_b(t) + V_c(t), \qquad (18)$$

where $V_a(t)$, $V_b(t)$ and $V_c(t)$ are defined as

$$\begin{aligned}V_a(t) &= \frac{1}{2}\beta\int_0^{H_f}\rho\{[\dot{w}_{1l}(y,t)]^2 + [\dot{w}_{1r}(y,t)]^2\}dy \\ &\quad +\frac{1}{2}\beta\int_{H_f}^{2H_f}\rho\{[\dot{w}_{2l}(y,t)]^2 + [\dot{w}_{2r}(y,t)]^2\}dy \\ &\quad +\frac{1}{2}\beta\int_0^{H_f}EI\{[w''_{1l}(y,t)]^2 + [w''_{1r}(y,t)]^2\}dy \\ &\quad +\frac{1}{2}\beta\int_0^{H_f}T\{[w'_{1l}(y,t)]^2 + [w'_{1r}(y,t)]^2\}dy \\ &\quad +\frac{1}{2}\beta\int_{H_f}^{2H_f}EI\{[w''_{2l}(y,t)]^2 + [w''_{2r}(y,t)]^2\}dy \\ &\quad +\frac{1}{2}\beta\int_{H_f}^{2H_f}T\{[w'_{2l}(y,t)]^2 + [w'_{2r}(y,t)]^2\}dy \\ &\quad +\frac{\beta}{2}M_f[\dot{w}_1(H_f,t)]^2 \qquad (19)\\ V_b(t) &= \frac{1}{2}\Big(M_c + \frac{(M_c+J_c)M_f}{J_c}\Big)[\mu(t)]^2 \qquad (20)\\ V_c(t) &= \alpha\rho\int_0^{H_f}y[\dot{w}_{2l}(y,t) + \dot{w}_{2r}(y,t)][w'_{2l}(y,t) \\ &\quad +w'_{2r}(y,t)]dy \qquad (21)\end{aligned}$$

where α and β both are positive constants.

The Lyapunov function candidate (18) has following Lemmas.

Lemma 1. The Lyapunov function candidate defined by (18) has upper and lower bounds and it is positive definite, namely,

$$0 \le \lambda_1(V_a(t) + V_b(t)) \le V(t) \le \lambda_2(V_a(t) + V_b(t)) \qquad (22)$$

where

$$\lambda_1 = 1 - \max\Big\{\frac{2\alpha\delta_1 H_f}{\beta}, \frac{2\alpha\rho H_f}{\delta_1\beta T}\Big\} \qquad (23)$$

$$\lambda_2 = 1 + \max\Big\{\frac{2\alpha\delta_1 H_f}{\beta}, \frac{2\alpha\rho H_f}{\delta_1\beta T}\Big\} \qquad (24)$$

and δ_1 is a positive constant.

Proof : See Appendix A.

Lemma 2. The first derivative of Lyapunov function candidate given by (18) satisfies $\dot{V}(t) \le 0$ and that $\dot{V}(t) = 0$ if and only if all states remain in zero.

Proof : See Appendix B.

On the basis of above Lemma 1 and Lemma 2, Theorem 1 is obtained.

Theorem 1. For the system described by (4)-(7) and boundary conditions (8)-(15), we can conclude that the high-rise building system with exact model-based boundary controller (17) is asymptotically stable.

Proof : Using the Lyapunov's direct method and Lemma 1 and Lemma 2, the asymptotical stability of the closed-loop system can be deducted. Then, using the Lemma 1 and Lemma 2, we can find that $V(t)$ can converge to zero as $t \to \infty$. Because the Lyapunov function candidate satisfies Lemma 1, i.e. $0 \le \lambda_1(V_a(t) + V_b(t)) \le V(t) \le \lambda_2(V_a(t) + V_b(t))$, every square term in $V(t)$ can converge to zero as $t \to \infty$.

B. Adaptive Boundary Control

For a high-rise building structure, its physical parameters, like EI, T and M_f, are difficult to be measured accurately. To deal with the parameter uncertainty, an adaptive boundary control is designed as follows.

$$\begin{aligned}u(t) &= -k\mu(t) - \frac{M_c+J_c}{J_c}\widehat{EI}(t)[w'''_{2r}(2H_f,t) \\ &\quad +w'''_{2l}(2H_f,t)] + \frac{M_c+J_c}{J_c}\hat{T}(t)[w'_{2l}(2H_f,t) \\ &\quad +w'_{2r}(2H_f,t)] + \gamma_1\Big(\frac{M_c+J_c}{J_c}\hat{M}_f(t) + M_c\Big) \\ &\quad \times[\dot{w}'''_{2l}(2H_f,t) + \dot{w}'''_{2r}(2H_f,t)] - \gamma_2\Big(\frac{M_c+J_c}{J_c} \\ &\quad \times\hat{M}_f(t) + M_c\Big)[\dot{w}'_{2l}(2H_f,t) + \dot{w}'_{2r}(2H_f,t)] \qquad (25)\end{aligned}$$

where $\widehat{EI}(t)$, $\hat{T}(t)$ and $\hat{M}_f(t)$ are the estimates of EI, T and M_f, respectively. The adaptation laws are designed as

$$\begin{aligned}\dot{\widehat{EI}}(t) &= \frac{M_c+J_c}{J_c\chi_1}[w'''_{2r}(2H_f,t) + w'''_{2l}(2H_f,t)]\mu(t) \qquad (26)\\ \dot{\hat{T}}(t) &= -\frac{M_c+J_c}{J_c\chi_2}[w'_{2l}(2H_f,t) + w'_{2r}(2H_f,t)]\mu(t) \qquad (27)\\ \dot{\hat{M}}_f(t) &= \gamma_2\frac{M_c+J_c}{J_c\chi_3}[\dot{w}'_{2l}(2H_f,t) + \dot{w}'_{2r}(2H_f,t)]\mu(t) \\ &\quad -\gamma_1\frac{M_c+J_c}{J_c\chi_3}[\dot{w}'''_{2l}(2H_f,t) + \dot{w}'''_{2r}(2H_f,t)]\mu(t) \qquad (28)\end{aligned}$$

where χ_1, χ_2 and χ_3 are positive constants.

Consider a modified Lyapunov function candidate as

$$E(t) = V(t) + \frac{\chi_1}{2}[\widetilde{EI}(t)]^2 + \frac{\chi_2}{2}[\tilde{T}(t)]^2 + \frac{\chi_3}{2}[\tilde{M}_f(t)]^2 \qquad (29)$$

where $\widetilde{EI}(t)$, $\tilde{T}(t)$ and $\tilde{M}_f(t)$ are the parameter estimate errors and they are defined as $\widetilde{EI}(t) = EI - \widehat{EI}(t)$, $\tilde{T}(t) = T - \hat{T}(t)$ and $\tilde{M}_f(t) = M_f - \hat{M}_f(t)$.

The Lyapunov candidate function (29) has following Lemmas.

Lemma 3. The Lyapunov function candidate defined by (29) has upper and lower bounds and it is positive definite.

Proof : Combining (29) and Property 1, we have

$$\begin{aligned} 0 \leq\ & \lambda_3\{V_a(t)+V_b(t)+\frac{\chi_1}{2}[\widetilde{EI}(t)]^2+\frac{\chi_2}{2}[\tilde{T}(t)]^2 \\ & +\frac{\chi_3}{2}[\tilde{M}_f(t)]^2\} \\ \leq\ & E(t) \\ \leq\ & \lambda_4\{V_a(t)+V_b(t)+\frac{\chi_1}{2}[\widetilde{EI}(t)]^2+\frac{\chi_2}{2}[\tilde{T}(t)]^2 \\ & +\frac{\chi_3}{2}[\tilde{M}_f(t)]^2\} \end{aligned} \tag{30}$$

where $\lambda_3=\min(\lambda_1,\frac{\chi_1}{2},\frac{\chi_2}{2},\frac{\chi_3}{2})$ and $\lambda_4=\max(\lambda_2,\frac{\chi_1}{2},\frac{\chi_2}{2},\frac{\chi_3}{2})$.

Lemma 4. The first derivative of Lyapunov function candidate given by (29) satisfies $\dot{E}(t)\leq 0$ and that $\dot{E}(t)=0$ if and only if all states remain in zero.

Proof : See Appendix C.

Theorem 2. For the system described by (4)-(7) and boundary conditions (8)-(15), we can conclude that the high-rise building system with adaptive boundary controller (25) and adaptation laws (26)-(28) is asymptotically stable.

Proof : Using the Lyapunov's direct method and Lemma 3 and Lemma 4, the asymptotical stability of the closed-loop system can be deducted. Then, using the Lemma 3 and Lemma 4, we can find that $V(t)$ can converge to zero as $t\to\infty$. Because the Lyapunov function candidate satisfies Lemma 3, i.e. $0\leq\lambda_1(V_a(t)+V_b(t))\leq V(t)\leq\lambda_2(V_a(t)+V_b(t))$, every square terms in $V(t)$ can converge to zero as $t\to\infty$.

IV. Numerical Simulation

This section will provide simulation results of the two-floor building plant with the exact model-based boundary controller (17) and the adaptive boundary controller (25), respectively. The initial state of the two-floor building plant is as follows.

$$w_{1l}(y,0) = 1.5y^4-2.275y^3+1.061y^2 \tag{31}$$
$$w_{1r}(y,0) = 2y^4-2.95y^3+1.280y^2 \tag{32}$$
$$w_{2l}(y,0) = 0.7y^4-0.756y^3+0.256y+0.079 \tag{33}$$
$$w_{2r}(y,0) = 0.9y^4-0.972y^3+0.288y+0.079 \tag{34}$$

The parameters of the building system are shown in Table 1.

Remark 2. The initial state is chose according to the boundary conditions (10)-(14). From the boundary conditions, we can find that the initial state need to satisfy the following conditions,

$$w_{1l}(0,0)=w_{1r}(0,0)=0 \tag{35}$$
$$w'_{1l}(0,0)=w'_{1r}(0,0)=0 \tag{36}$$
$$w''_{1l}(H_f,0)=w''_{1r}(H_f,0)=0 \tag{37}$$
$$w'_{2l}(H_f,0)=w'_{2r}(H_f,0)=0 \tag{38}$$
$$w''_{2l}(2H_f,0)=w''_{2r}(2H_f,0)=0 \tag{39}$$

TABLE I
THE PHYSICAL PARAMETERS OF THE BUILDING SYSTEM IN THE SIMULATIONS

Parameter	Value	Unit
M_c	0.65	kg
J_c	0.133	kg.m^2
L	0.54	m
ρ	0.453	kg/m
M_f	0.68	kg
EI	25 $(0\sim 2s)$	N.m^2
	20 $(2\sim 7s)$	N.m^2
	30 $(7\sim 10s)$	N.m^2
T	440 $(0\sim 2s)$	N
	435 $(2\sim 7s)$	N
	500 $(7\sim 10s)$	N

Based upon the analyzing of the above conditions, we can find that if the initial state is chosen as polynomial functions, the order of those functions must more than three. Then by analyzing different initial states, we choose the initial state which looks the most similar with the real experiment platform.

A. Simulation Results for the Building Plant without Control

When the high-rise plant without control vibrates under the aforementioned initial condition, the displacements and the accelerations of first and second floors cannot converge to zero (Fig. 3). In Fig. 3, the x-axes denote the time, and the y-axes denote the accelerations of the first and the second floors ($\ddot{w}_1(H_f,t)$ and $\ddot{w}_2(2H_f,t)$) and the displacements of the first and the second floors ($w_1(H_f,t)$ and $w_2(2H_f,t)$).

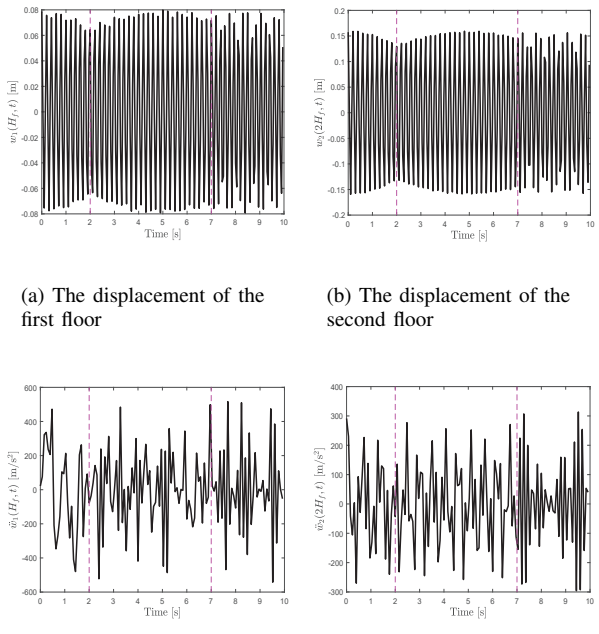

(a) The displacement of the first floor

(b) The displacement of the second floor

(c) The acceleration of the first floor

(d) The acceleration of the seconde floor

Fig. 3. The building plant system without control.

B. Simulation Results for the Building Plant with Model-Based Boundary Control

The simulation results of the building system with exact

model-based boundary control are shown in Fig. 4. The control gains are $\gamma_1 = 0.013$, $\gamma_2 = 0.44$ and $k = 3.5$. Fig. 4(a) and Fig. 4(b) show the displacements of the first and second floor respectively. Fig. 4(c) and Fig. 4(d) show the accelerations of the first and second floor respectively. In the range of $0 \sim 2$ seconds, $EI = 25\text{Nm}^2$, $T = 440\text{N}$, and $M_f = 0.68\text{kg}$, the exact model-based boundary controller enables the displacements and the accelerations of first and second floors to be suppressed within 1.5s. However, in the range of $2 \sim 7$ seconds, when the parameters change to $EI = 20\text{Nm}^2$, $T = 435\text{N}$, and $M_f = 0.68\text{kg}$, the displacements and accelerations of the building system jump greatly or even be impossible to converge to a small range. Then, in the range of $7 \sim 10$ seconds, $EI = 30\text{Nm}^2$, $T = 500\text{N}$, and $M_f = 0.68\text{kg}$, the displacements and the accelerations of the building system with model-based boundary control can converge to zero, but both the displacements and accelerations have overshoot. Hence, the change of system parameters has great influence on exact model-based control. Exact model-based control cannot deal with the condition that the physical parameters of high-rise buildings are unknown or variational.

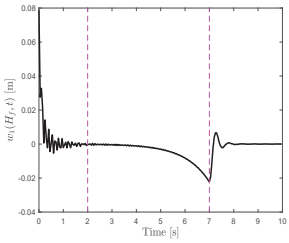

(a) The displacement of the first floor

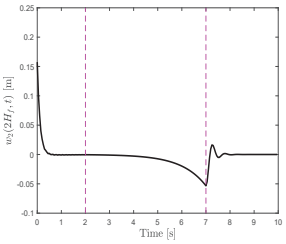

(b) The displacement of the second floor

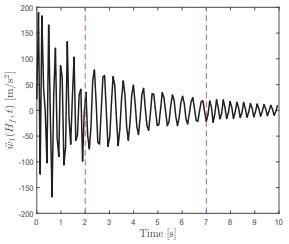

(c) The acceleration of the first floor

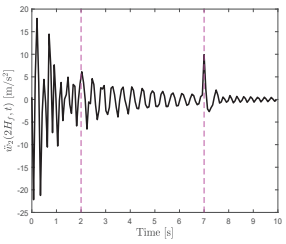

(d) The acceleration of the seconde floor

Fig. 4. The building plant system with exact model-based boundary control.

C. Simulation Results for the Building Plant with Adaptive Boundary Control

The adaptive boundary control law is used in the building plant to deal with the uncertainty of the physical parameters. The control gains are $\gamma_1 = 0.033$, $\gamma_2 = 1.17$ and $k = 3.5$, and the adaptive parameters are $\chi_1 = 0.0000023$, $\chi_2 = 0.0001$ and $\chi_3 = 8.5$. Fig. 5 and Fig. 6 show the displacements of the left and right walls of the the whole building respectively. In Fig. 5 and Fig. 6, the x-axes denote the time; the y-axes mean the hight of the building; the z-axes denote the displacements. Fig. 7(a) and Fig. 7(b) show the displacements of the first and second floor respectively. Fig. 7(c) and Fig. 7(d) show the accelerations of the first and second floor respectively. From Fig. 5 - Fig. 7, we can find that the adaptive boundary controller enables that the building system has stable and good control effects when the physical parameters change in the range of $2 \sim 7$ seconds and $7 \sim 10$ seconds, although the converge time of building system with the adaptive boundary controller is longer than with the exact model-based controller. Moreover, the converge time is not a big deal, because the converge time is just 2.0 seconds. Hence, the change of system parameters cannot exert a great influence on adaptive boundary control. Adaptive boundary control can deal with the condition that the physical parameters of high-rise buildings are unknown or variational efficiently.

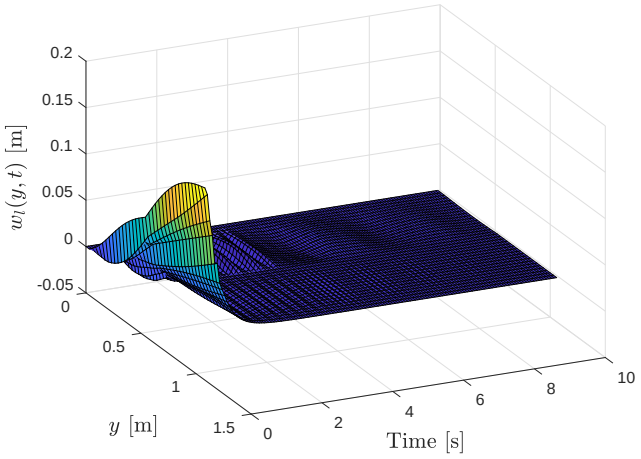

Fig. 5. The displacement of the left wall with adaptive boundary control.

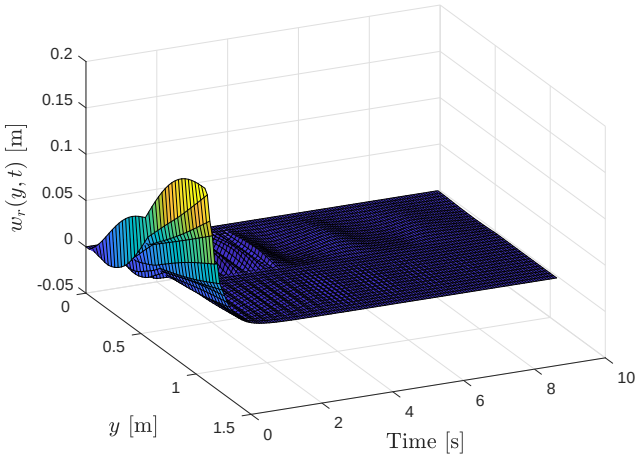

Fig. 6. The displacement of the right wall with adaptive boundary control.

Moreover, for quantitatively analyzing, Table 2 presents the root-mean-square(RMS) values of the displacements and the accelerations of the building system, where the simulations (a), (b) and (c) mean the building system has no control,

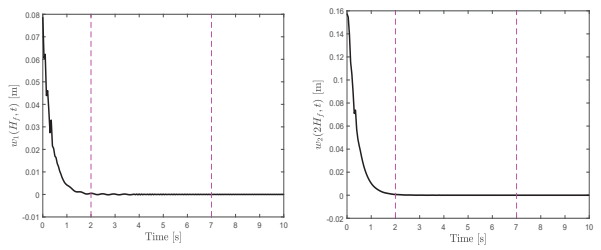

(a) The displacement of the first floor

(b) The displacement of the second floor

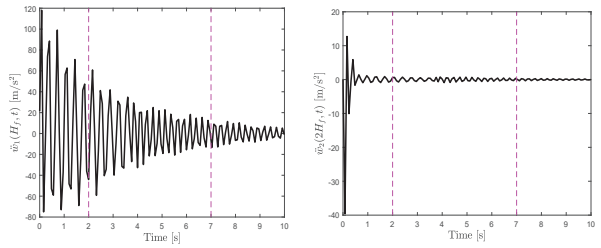

(c) The acceleration of the first floor

(d) The acceleration of the seconde floor

Fig. 7. The building plant system with adaptive boundary control.

TABLE II
THE COMPARISON WITH ROOT-MEAN-SQUARE VALUE IN THE SIMULATIONS

	Displacement		Acceleration	
	$w_1(H_f,t)$ [m]	$w_2(2H_f,t)$ [m]	$\ddot{w}_1(H_f,t)$ [m/s^2]	$\ddot{w}_2(2H_f,t)$ [m/s^2]
(a)	0.0545	0.1117	232.3180	148.5863
(b)	0.0076	0.0176	51.3506	74.2390
(c)	0.0100	0.0241	34.5350	11.5332

has exact model-based control and has adaptive boundary control, respectively. Comparing with the no control state, exact model-based control and adaptive boundary both has small RMS values. For displacement, the RMS value of the exact model-based controller is about 33% smaller than the adaptive boundary controller. But combining the Fig. 4 and Fig. 7, we can find that the RMS values for displacement should not be considered because of the bad performance of the exact model-based controller when the physical parameters are changing. Then, for acceleration, the RMS value of the exact model-based controller is over 50% bigger than the adaptive boundary controller. Especially for the acceleration of the second floor, the RMS value of the exact model-based controller is over 6.5 times the RMS value of the adaptive boundary controller.

From the simulations in Part A, B and C and the analysis of Table 2, we can summarize that the adaptive boundary control strategy can improve the performance of exact model-based boundary control strategy. Adaptive boundary control can also solve the problem that the parameters of buildings are difficult to be measured and change frequently.

Remark 3. When the parameters EI and T change in the model, the parameters EI and T used in the exact model-based controller remain in 25 N.m^2 and 440 N. These simulations simulate the changes of physical parameters in a long period, which is slow process in practice. The derivative of the parameters (EI, T) with respect to time is near zero, i.e. $\dot{EI} \approx 0$, $\dot{T} \approx 0$.

V. EXPERIMENTS

Using the experiments on the Quanser's building platform, this section will verify the feasibility of the adaptive boundary controller and the exact model-based boundary controller. The physical parameters of the Quanser's platform are shown in Table III. The excitation signals are provided by external force which can make the top floor of the building platform move 5cm.

TABLE III
THE PHYSICAL PARAMETERS OF QUANSER'S HIGH-RISE BUILDING SYSTEM

Description	Value	Unit
Flexible Module Length	0.32	m
Flexible Module Height	0.5	m
Flexible Module Depth	0.11	m
Structure Top Floor Height	1.06	m
Structure Floor Mass	0.68	kg
Cart Mass	0.39	kg
Cart Rotor Moment of Inertia	$3.90E-7$	kg.m^2
Cart Planetary Gearbox Gear Ratio	3.71	
Cart Motor Pinion Radius	$6.35E-3$	m

As shown in Fig. 8, the control laws are written in Simulink on computer, then transmitted to the data acquisition device by USB. The VoltPAQ-X1 amplifier convert the digital control signal to analog signal for controlling the cart on the top floor. At the same time, the data acquisition device receives the sensor signals from the building platform, and sends the immediate sensor signals to computer.

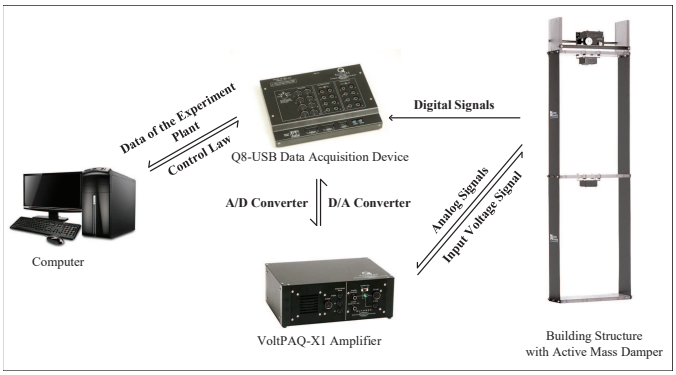

Fig. 8. The working principle of the Quanser's building platform.

During the experiments, we give a disturbance which can make the top floor move 5cm. The control gains of the exact model-based boundary controller and the adaptive boundary controller are $k = 9$, $\gamma_1 = 0.05$, and $\gamma_2 = 50$. The value of the adaptive parameters is $\chi_1 = 0.000002$, $\chi_2 = 0.0001$, $\chi_3 = 9$. Fig. 9 to Fig. 11 show the control effect when the building system has no control, boundary control and

adaptive boundary control, respectively. From Fig. 9, we can find that, the building platform without control can suppress the vibration slowly with the help of damping. From Fig. 10 and Fig. 11, we can find that, the building platform with model-based control and adaptive control both can suppress the vibration within 2.5s. And the adaptive boundary control method can present a better control effect on acceleration. But when the physical parameters cannot be known exactly, the adaptive boundary control can also reach a stable and good control effect. In addition, for quantitatively analyzing, the root-mean-square value of the displacement and acceleration in above three experiments is shown in Table 4 where the experiments (a), (b) and (c) denote the experiments without control, with exact model-based boundary control and with adaptive boundary control, respectively. Comparing with the no control state, the RMS values of the displacement of the two control states are smaller. The RMS values of the displacement of the adaptive control state are smaller than the exact model-based control state, which is different with the simulation results. For acceleration, the RMS values of the first floor of the two control states are smaller than the no control state, but the RMS values of the second floor of the two control states are bigger than the no control state. Combining with the Fig. 9-Fig. 11, we can find that this situation is caused by the spines at the beginning of acting of the controller. To sum up, from the Table 4, we can also find that the building system with adaptive control has a smaller RMS value than the building system with exact model-based control, and the adaptive boundary controller has better control effect than the exact model-based controller.

TABLE IV
THE COMPARISON WITH ROOT-MEAN-SQUARE VALUE IN THE EXPERIMENTS

	Displacement		Acceleration	
	$w_1(H_f,t)$ [m]	$w_2(2H_f,t)$ [m]	$\ddot{w}_1(H_f,t)$ [m/s^2]	$\ddot{w}_2(2H_f,t)$ [m/s^2]
(a)	0.0138	0.0099	0.5913	0.5489
(b)	0.0102	0.0079	0.5744	0.9205
(c)	0.0091	0.0069	0.4588	0.9205

VI. CONCLUSION

In this paper, a two-storey building platform is modeled as a partial differential equation model which guarantees that infinite characters can be reserved in the model. Then a boundary controller and an adaptive boundary controller are presented in order to suppress the vibration of the building platform, and to adapt the changes of physical parameters of the building structure, like EI, T and M_f. By using the Lyapunov's direct method, the asymptotical stability of the closed-loop building system is proved. Besides, the simulations and the experiments illustrate the adaptivity and effectiveness of the adaptive boundary control by comparing with exact model-based boundary control.

Based on the work in this paper which mainly deals with the vibration suppression and parameters' uncertainty of a two-storey building, we plan to extend the adaptive control method to finite-time control [43], [44], and be used in an N-storey building model in the future.

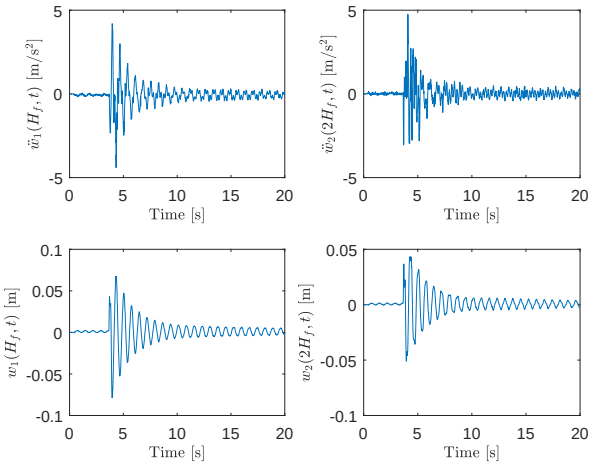

Fig. 9. The control effect of the building system without control.

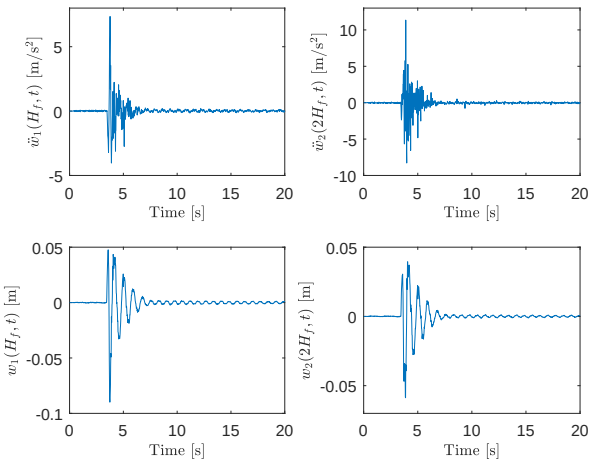

Fig. 10. The control effect of the building system with model-based boundary control.

REFERENCES

[1] J. T. P. Yao, "Concept of structural control," *Asce Journal of the Structural Division*, vol. 98, no. 7, pp. 1567–1574, 1972.
[2] L. L. Chung, Y. A. Lai, C. S. W. Yang, K. H. Lien, and L. Y. Wu, "Semi-active tuned mass dampers with phase control," *Journal of Sound & Vibration*, vol. 332, no. 15, pp. 3610–3625, 2013.
[3] H.-B. Xu, C.-W. Zhang, H. Li, P. Tan, J.-P. Ou, and F.-L. Zhou, "Active mass driver control system for suppressing wind-induced vibration of the canton tower," *Smart Structures & Systems*, vol. 13, no. 2, pp. 281–303, 2014.
[4] K. Ghaedi, Z. Ibrahim, H. Adeli, and A. Javanmardi, "Invited review: Recent developments in vibration control of building and bridge structures," *Journal of Vibroengineering*, vol. 19, no. 5, pp. 3564–3580, 2017.
[5] S. Paul, W. Yu, and X. Li, "Recent advances in bidirectional modeling and structural control," *Shock & Vibration*, vol. 2016, pp. 1–17, 2016.
[6] T. Soong and B. Spencer Jr, "Supplemental energy dissipation: state-of-the-art and state-of-the-practice," *Engineering Structures*, vol. 24, no. 3, pp. 243–259, 2002.

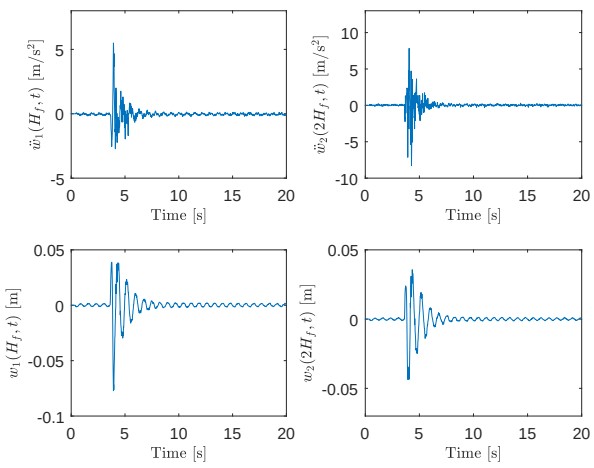

Fig. 11. The control effect of the building system with adaptive boundary control.

[7] M. Zeinali, S. A. Mazlan, A. Y. A. Fatah, and H. Zamzuri, "A phenomenological dynamic model of a magnetorheological damper using a neuro-fuzzy system," *Smart Materials & Structures*, vol. 22, no. 12, p. 125013, 2013.

[8] M. Morales-Beltran and J. Paul, "Technical note: Active and semi-active strategies to control building structures under large earthquake motion," *Journal of Earthquake Engineering*, vol. 19, no. 7, pp. 1086–1111, 2015.

[9] C. M. Chang, S. Shia, and Y. A. Lai, "Seismic design of passive tuned mass damper parameters using active control algorithm," *Journal of Sound & Vibration*, vol. 426, pp. 150–165, 2018.

[10] N. Wang and H. Adeli, "Robust vibration control of wind-excited high-rise building structures," *Journal of Civil Engineering & Management*, vol. 21, no. 8, pp. 967–976, 2015.

[11] C.-J. Chen and S.-M. Yang, "Application neural network controller and active mass damper in structural vibration suppression," *Journal of Intelligent & Fuzzy Systems*, vol. 27, no. 6, pp. 2835–2845, 2014.

[12] M. Soleymani and M. Khodadadi, "Adaptive fuzzy controller for active tuned mass damper of a benchmark tall building subjected to seismic and wind loads," *The Structural Design of Tall & Special Buildings*, vol. 23, no. 10, pp. 781–800, 2014.

[13] W. He and S. S. Ge, "Cooperative control of a nonuniform gantry crane with constrained tension," *Automatica*, vol. 66, pp. 146–154, 2016.

[14] Z. Zhao, Y. Liu, F. Guo, and Y. Fu, "Vibration control and boundary tension constraint of an axially moving string system," *Nonlinear Dynamics*, vol. 89, no. 1, pp. 1–10, 2017.

[15] K. Morris, "The role of sensor and actuator models in control of distributed parameter systems," in *Emerging Applications of Control & Systems Theory*, pp. 245–257, Springer, 2018.

[16] X. He, W. He, J. Shi, and C. Sun, "Boundary vibration control of variable length crane systems in two-dimensional space with output constraints," *IEEE/ASME Transactions on Mechatronics*, vol. 22, no. 5, pp. 1952–1962, 2017.

[17] W. He, Y. Ouyang, and J. Hong, "Vibration control of a flexible robotic manipulator in the presence of input deadzone," *IEEE Transactions on Industrial Informatics*, vol. 13, no. 1, pp. 48–59, 2016.

[18] Y. Guo and J. Wang, "Stabilization of a non-homogeneous rotating body-beam system with the torque and nonlinear distributed controls," *Journal of Systems Science & Complexity*, vol. 30, no. 3, pp. 616–626, 2017.

[19] W. He and S. Zhang, "Control design for nonlinear flexible wings of a robotic aircraft," *IEEE Transactions on Control Systems Technology*, vol. 25, no. 1, pp. 351–357, 2016.

[20] Z.-J. Han and G.-Q. Xu, "Output-based stabilization of Euler-Bernoulli beam with time-delay in boundary input," *IMA journal of Mathematical Control & Information*, vol. 31, no. 4, pp. 533–550, 2014.

[21] Z. Liu, J. Liu, and W. He, "Modeling and vibration control of a flexible aerial refueling hose with variable lengths and input constraint," *Automatica*, vol. 77, pp. 302–310, 2017.

[22] S. Feng and H.-N. Wu, "Hybrid robust boundary and fuzzy control for disturbance attenuation of nonlinear coupled ODE-beam systems with application to a flexible spacecraft," *IEEE Transactions on Fuzzy Systems*, vol. 25, no. 5, pp. 1293–1305, 2016.

[23] Y. Liu, Y. Fu, W. He, and Q. Hui, "Modeling and observer-based vibration control of a flexible spacecraft with external disturbances," *IEEE Transactions on Industrial Electronics*, vol. 66, no. 11, pp. 8648–8658, 2019.

[24] K. D. Do and J. Pan, "Boundary control of transverse motion of marine risers with actuator dynamics," *Journal of Sound & Vibration*, vol. 318, no. 4, pp. 768–791, 2008.

[25] S. K. Chakrabarti and R. E. Frampton, "Review of riser analysis techniques," *Applied Ocean Research*, vol. 4, no. 2, pp. 73–90, 1982.

[26] Z. Zhao, X. He, Z. Ren, and G. Wen, "Boundary adaptive robust control of a flexible riser system with input nonlinearities," *IEEE Transactions on Systems, Man, and Cybernetics: Systems*, vol. In press, 2018.

[27] Z. Yang, M. Krstic, and H. Su, "PDE boundary control of multi-input LTI systems with distinct and uncertain input delays," *IEEE Transactions on Automatic Control*, vol. 63, no. 12, pp. 4270–4277, 2018.

[28] T. Meurer and A. Kugi, "Tracking control for boundary controlled parabolic PDEs with varying parameters: Combining backstepping and differential flatness ," *Automatica*, vol. 45, no. 5, pp. 1182–1194, 2009.

[29] Y. Tan, H.-H. Dai, D. Huang, and J.-X. Xu, "Unified iterative learning control schemes for nonlinear dynamic systems with nonlinear input uncertainties," *Automatica*, vol. 48, no. 12, pp. 3173–3182, 2012.

[30] W. He, T. Meng, D. Huang, and X. Li, "Adaptive boundary iterative learning control for an Euler–Bernoulli beam system with input constraint," *IEEE Transactions on Neural Networks and Learning Systems*, vol. 29, no. 5, pp. 1539–1549, 2017.

[31] C. Sun, W. He, and J. Hong, "Neural network control of a flexible robotic manipulator using the lumped spring-mass model," *IEEE Transactions on Systems, Man, and Cybernetics: Systems*, vol. 47, no. 8, pp. 1863–1874, 2016.

[32] W. He and Y. Dong, "Adaptive fuzzy neural network control for a constrained robot using impedance learning," *IEEE Transactions on Neural Networks and Learning Systems*, vol. 29, no. 4, pp. 1174–1186, 2017.

[33] H. N. Wu, J.-W. Wang, and H.-X. Li, "Fuzzy boundary control design for a class of nonlinear parabolic distributed parameter systems," *IEEE Transactions on Fuzzy Systems*, vol. 22, no. 3, pp. 642–652, 2014.

[34] M. Krstic, *Boundary control of PDEs: A course on backstepping designs*. Philadelphia, USA: Siam, 2008.

[35] Y. Liu, F. Guo, X. He, and Q. Hui, "Boundary control for an axially moving system with input restriction based on disturbance observers," *IEEE Transactions on Systems, Man, and Cybernetics: Systems*, vol. 49, no. 11, pp. 2242–2253, 2019.

[36] F.-F. Jin and B.-Z. Guo, "Performance boundary output tracking for one-dimensional heat equation with boundary unmatched disturbance," *Automatica*, vol. 96, pp. 1–10, 2018.

[37] Z. Liu, Z. Zhao, and C. K. Ahn, "Boundary constrained control of flexible string systems subject to disturbances," *IEEE Transactions on Circuits and Systems II: Express Briefs*, vol. In press, 2019.

[38] T. Meng, H. Wei, Y. Hong, J. K. Liu, and Y. Wei, "Vibration control for a flexible satellite system with output constraints," *Nonlinear Dynamics*, vol. 85, no. 4, pp. 1–14, 2016.

[39] T. Endo, F. Matsuno, and Y. Jia, "Boundary cooperative control by flexible Timoshenko arms," *Automatica*, vol. 81, pp. 377–389, 2017.

[40] G. Xie, L. Sun, T. Wen, X. Hei, and F. Qian, "Adaptive transition probability matrix-based parallel IMM algorithm," *IEEE Transactions on Systems, Man, and Cybernetics: Systems*, vol. In press, 2019.

[41] W. He, Z. Li, Y. Dong, and T. Zhao, "Design and adaptive control for an upper limb robotic exoskeleton in presence of input saturation," *IEEE Transactions on Neural Networks and Learning Systems*, vol. 30, no. 1, pp. 97–108, 2018.

[42] Q. C. Nguyen and K.-S. Hong, "Asymptotic stabilization of a nonlinear axially moving string by adaptive boundary control," *Journal of Sound & Vibration*, vol. 329, no. 22, pp. 4588–4603, 2010.

[43] H. Li, S. Zhao, W. He, and R. Lu, "Adaptive finite-time tracking control of full state constrained nonlinear systems with dead-zone," *Automatica*, vol. 100, pp. 99–107, 2019.

[44] P. Du, H. Liang, S. Zhao, and C. K. Ahn, "Neural-based decentralized adaptive finite-time control for nonlinear large-scale systems with time-varying output constraints," *IEEE Transactions on Systems, Man, and Cybernetics: Systems*, vol. In press, 2019.

APPENDICES

A. PROOF OF PROPERTY 1

Proof: By using the Young's inequality to $V_c(t)$, we have

$$\begin{aligned}|V_c(t)| \leq\ & \alpha\rho H_f \int_0^{H_f} \frac{\delta_1}{2}[\dot{w}_{2l}(y,t)+\dot{w}_{2r}(y,t)]^2 dy \\ & +\alpha\rho H_f \int_0^{H_f} \frac{1}{2\delta_1}[w'_{2l}(y,t)+w'_{2r}(y,t)]^2 dy \\ \leq\ & \alpha\rho H_f \int_0^{H_f} \delta_1[\dot{w}_{2l}(y,t)]^2 dy \\ & +\alpha\rho H_f \int_0^{H_f} \delta_1[\dot{w}_{2r}(y,t)]^2 dy \\ & +\alpha\rho H_f \int_0^{H_f} \frac{1}{\delta_1}[w'_{2l}(y,t)]^2 dy \\ & +\alpha\rho H_f \int_0^{H_f} \frac{1}{\delta_1}[w'_{2r}(y,t)]^2 dy \\ \leq\ & \mu_1 V_a(t), \end{aligned} \tag{A.1}$$

where δ_1 is a positive constant and

$$\mu_1 = \max\Big\{\frac{2\alpha\delta_1 H_f}{\beta}, \frac{2\alpha\rho H_f}{\delta_1\beta T}\Big\} \tag{A.2}$$

Therefore, we have $-\mu_1 V_a(t) \leq V_c(t) \leq \mu_1 V_a(t)$. When μ_1 satisfies $0<\mu_1<1$, we further have

$$0 \leq \lambda_1(V_a(t)+V_b(t)) \leq V(t) \leq \lambda_2(V_a(t)+V_b(t)). \tag{A.3}$$

where $\lambda_1 = 1-\mu_1$ and $\lambda_2 = 1+\mu_1$.

B. PROOF OF PROPERTY 2

Proof: Taking the derivative of (18) with respect to time, we have

$$\dot{V}(t) = \dot{V}_a(t) + \dot{V}_b(t) + \dot{V}_c(t) \tag{B.1}$$

Substituting the motion equations (4) to (7), and integrating by part, the first term of (B.1) can be written as

$$\begin{aligned}\dot{V}_a(t) =\ & -\beta EI w'''_{2l}(2H_f,t)\dot{w}_{2l}(2H_f,t) \\ & -\beta EI w'''_{2r}(2H_f,t)\dot{w}_{2r}(2H_f,t) \\ & +\beta T w'_{2l}(2H_f,t)\dot{w}_{2l}(2H_f,t) \\ & +\beta T w'_{2r}(2H_f,t)\dot{w}_{2r}(2H_f,t) \\ =\ & -\frac{\beta\gamma_1 EI}{2}\{[w'''_{2l}(2H_f,t)+w'''_{2r}(2H_f,t)]\}^2 \\ & -\frac{\beta{\gamma_2}^2 EI}{2\gamma_1}\{[w'_{2l}(2H_f,t)+w'_{2r}(2H_f,t)]\}^2 \\ & -\frac{\beta EI}{2\gamma_1}[\dot{w}_2(2H_f,t)]^2 + \beta\gamma_2 EI[w'''_{2l}(2H_f,t) \\ & +w'''_{2r}(2H_f,t)][w'_{2l}(2H_f,t)+w'_{2r}(2H_f,t)] \\ & +\frac{\beta EI}{2\gamma_1}[\mu(t)]^2 - \frac{\beta\gamma_2 EI}{\gamma_1}\dot{w}_2(2H_f,t) \\ & \times[w'_{2l}(2H_f,t)+w'_{2r}(2H_f,t)] \end{aligned} \tag{B.2}$$

In addition, the terms $-\frac{\beta\gamma_2 EI}{\gamma_1}\dot{w}_2(2H_f,t)[w'_{2l}(2H_f,t)+w'_{2r}(2H_f,t)]$ and $\beta\gamma_2 EI[w'''_{2l}(2H_f,t)+w'''_{2r}(2H_f,t)][w'_{2l}(2H_f,t)+w'_{2r}(2H_f,t)]$ satisfy following inequalities, respectively.

$$\begin{aligned}& |-\frac{\beta\gamma_2 EI}{\gamma_1}\dot{w}_2(2H_f,t)[w'_{2l}(2H_f,t)+w'_{2r}(2H_f,t)]| \\ \leq\ & \frac{\beta\gamma_2 EI\delta_2}{2\gamma_1}[\dot{w}_2(2H_f,t)]^2 \\ & +\frac{\beta\gamma_2 EI}{2\gamma_1\delta_2}[w'_{2l}(2H_f,t)+w'_{2r}(2H_f,t)]^2 \end{aligned} \tag{B.3}$$

$$\begin{aligned}& |EI\beta\gamma_2[w'''_{2l}(2H_f,t)+w'''_{2r}(2H_f,t)][w'_{2l}(2H_f,t) \\ & +w'_{2r}(2H_f,t)]| \\ \leq\ & \frac{EI\beta\gamma_2\delta_3}{2}[w'''_{2l}(2H_f,t)+w'''_{2r}(2H_f,t)]^2 \\ & +\frac{EI\beta\gamma_2}{2\delta_3}[w'_{2l}(2H_f,t)+w'_{2r}(2H_f,t)]^2 \end{aligned} \tag{B.4}$$

where δ_2 and δ_3 are positive constants. Using the boundary conditions (8) and (15), and the boundary control law (17), the second term of (B.1) can be written as

$$\begin{aligned}\dot{V}_b(t) =\ & \Big(M_c+\frac{(M_c+J_c)M_f}{J_c}\Big)\mu(t)\dot{\mu}(t) \\ =\ & \mu(t)\Big\{\frac{M_c+J_c}{J_c}EI[w'''_{2l}(2H_f,t)+w'''_{2r}(2H_f,t)] \\ & -\frac{M_c+J_c}{J_c}T[w'_{2l}(2H_f,t)+w'_{2r}(2H_f,t)] \\ & -\Big(M_c+\frac{(M_c+J_c)M_f}{J_c}\Big)[\gamma_1\dot{w}'''_{2l}(2H_f,t) \\ & +\gamma_1\dot{w}'''_{2r}(2H_f,t)-\gamma_2\dot{w}'_{2l}(2H_f,t) \\ & -\gamma_2\dot{w}'_{2r}(2H_f,t)]+u(t)\Big\} \\ =\ & -k[\mu(t)]^2 \end{aligned} \tag{B.5}$$

Substituting the motion equations (6) and (7), and integrating by part, the third term of (B.1) can be written as

$$\begin{aligned}\dot{V}_c(t) =\ & \alpha\rho\int_{H_f}^{2H_f} y[\ddot{w}_{2l}(y,t)+\ddot{w}_{2r}(y,t)][w'_{2l}(y,t) \\ & +w'_{2r}(y,t)]dy+\alpha\rho\int_{H_f}^{2H_f} y[\dot{w}_{2l}(y,t) \\ & +\dot{w}_{2r}(y,t)][\dot{w}'_{2l}(y,t)+\dot{w}'_{2r}(y,t)]dy \\ =\ & -2\alpha EIH_f[w'''_{2l}(2H_f,t)+w'''_{2r}(2H_f,t)] \\ & \times[w'_{2l}(2H_f,t)+w'_{2r}(2H_f,t)] \\ & -\frac{3\alpha}{2}EI\int_{H_f}^{2H_f}[w''_{2l}(y,t)+w''_{2r}(y,t)]^2 dy \\ & +\alpha TH_f[w'_{2l}(2H_f,t)+w'_{2r}(2H_f,t)]^2 \\ & -\frac{\alpha}{2}TH_f[w'_{2l}(H_f,t)+w'_{2r}(H_f,t)]^2 \\ & -\frac{\alpha}{2}T\int_{H_f}^{2H_f}[w'_{2l}(y,t)+w'_{2r}(y,t)]^2 dy \\ & +2\alpha\rho H_f[\dot{w}_2(2H_f,t)]^2 - 2\alpha\rho H_f[\dot{w}(H_f,t)]^2 \\ & -\frac{\alpha}{2}\rho\int_{H_f}^{2H_f}[\dot{w}_{2l}(y,t)+\dot{w}_{2r}(y,t)]^2 dy \end{aligned} \tag{B.6}$$

The term $-2\alpha EIH_f[w_{2l}'''(2H_f,t) + w_{2r}'''(2H_f,t)] \times[w_{2l}'(2H_f,t) + w_{2r}'(2H_f,t)]$ satisfies following inequality

$$\begin{aligned}
&|-2EI\alpha H_f[w_{2l}'''(2H_f,t) + w_{2r}'''(2H_f,t)][w_{2l}'(2H_f,t) \\
&+w_{2r}'(2H_f,t)]| \\
\leq\ & EI\alpha H_f\delta_4[w_{2l}'''(2H_f,t) + w_{2r}'''(2H_f,t)]^2 \\
&+\frac{EI\alpha H_f}{\delta_4}[w_{2l}'(2H_f,t) + w_{2r}'(2H_f,t)]^2 \qquad \text{(B.7)}
\end{aligned}$$

where δ_4 is a positive constant. Using equations (B.2) to (B.7), we can obtain

$$\begin{aligned}
\dot{V}(t) \leq\ & -(\frac{\beta EI}{2\gamma_1} - 2\alpha\rho H_f - \frac{\beta\gamma_2 EI\delta_2}{2\gamma_1})[\dot{w}_2(2H_f,t)]^2 \\
& -EI(\frac{\beta\gamma_1}{2} - \frac{\beta\gamma_2\delta_3}{2} - \alpha H_f\delta_4)[w_{2l}'''(2H_f,t) \\
& +w_{2r}'''(2H_f,t)]^2 - (\frac{\beta{\gamma_2}^2 EI}{2\gamma_1} - \frac{\beta\gamma_2 EI}{2\gamma_1\delta_2} \\
& -\frac{EI\beta\gamma_2}{2\delta_3} - \frac{EI\alpha H_f}{\delta_4} - \frac{\alpha}{2}TH_f)[w_l'(2H_f,t) \\
& +w_r'(2H_f,t)]^2 - 2\alpha\rho H_f[\dot{w}(H_f,t)]^2 \\
& -\frac{3\alpha}{2}EI\int_{H_f}^{2H_f}[w_{2l}''(y,t) + w_{2r}''(y,t)]^2dy \\
& -\frac{\alpha}{2}T\int_{H_f}^{2H_f}[w_{2l}'(y,t) + w_{2r}'(y,t)]^2dy \\
& -\frac{\alpha}{2}\rho\int_{H_f}^{2H_f}[\dot{w}_{2l}(y,t) + \dot{w}_{2r}(y,t)]^2dy \\
& -(k - \frac{\beta EI}{2\gamma_1})[\mu(t)]^2 \qquad \text{(B.8)}
\end{aligned}$$

where the positive constants $\alpha, \beta, \gamma_1, \gamma_2, \delta_2, \delta_3, \delta_4$ and k are chosen under the following conditions.

$$\sigma_1 = k - \frac{\beta EI}{2\gamma_1} > 0, \qquad \text{(B.9)}$$

$$\sigma_2 = \frac{\beta EI}{2\gamma_1} - 2\alpha\rho H_f - \frac{\beta\gamma_2 EI\delta_2}{2\gamma_1} > 0 \qquad \text{(B.10)}$$

$$\sigma_3 = \frac{\beta\gamma_1}{2} - \frac{\beta\gamma_2\delta_3}{2} - \alpha H_f\delta_4 > 0 \qquad \text{(B.11)}$$

$$\begin{aligned}
\sigma_4 =\ & \frac{\beta{\gamma_2}^2 EI}{2\gamma_1} - \frac{\beta\gamma_2 EI}{2\gamma_1\delta_2} - \frac{EI\beta\gamma_2}{2\delta_3} \\
& -\frac{EI\alpha H_f}{\delta_4} - \frac{\alpha}{2}TH_f > 0 \qquad \text{(B.12)}
\end{aligned}$$

From (B.8), we have $\dot{V}(t)$ is negative semidefinite. When $\dot{V}(t) \equiv 0$, we can obtain $w_{2l}''(y,t) + w_{2r}''(y,t) = 0$, $w_{2l}'(y,t) + w_{2r}'(y,t) = 0$, $\dot{w}_{2l}(y,t) + \dot{w}_{2r}(y,t) = 0$, $\mu(t) = 0$, $\dot{w}(H_f,t) = 0$, $\dot{w}_2(2H_f,t) = 0$, $w_{2l}'''(2H_f,t) + w_{2r}'''(2H_f,t) = 0$, $w_{2l}'(2H_f,t) + w_{2r}'(2H_f,t) = 0$, the dynamic model can be rewritten as

$$\rho\ddot{w}_{1l}(y,t) + EIw_{1l}''''(y,t) - Tw_{1l}''(y,t) = 0 \qquad \text{(B.13)}$$

$$\rho\ddot{w}_{1r}(y,t) + EIw_{1r}''''(y,t) - Tw_{1r}''(y,t) = 0 \qquad \text{(B.14)}$$

$$\rho\ddot{w}_{2l}(y,t) + EIw_{2l}''''(y,t) - Tw_{2l}''(y,t) = 0 \qquad \text{(B.15)}$$

$$\rho\ddot{w}_{2r}(y,t) + EIw_{2r}''''(y,t) - Tw_{2r}''(y,t) = 0 \qquad \text{(B.16)}$$

$$\dot{w}_2(2H_f,t) = 0 \qquad \text{(B.17)}$$

$$\dot{w}_1(H_f,t) = 0 \qquad \text{(B.18)}$$

$$\begin{aligned}
&-EI[w_{1l}'''(H_f,t) + w_{1r}'''(H_f,t)] \\
&+T[w_{1l}'(H_f,t) + w_{1r}'(H_f,t)] = 0 \qquad \text{(B.19)}
\end{aligned}$$

$$w_{1l}(0,t) = w_{1r}(0,t) = 0 \qquad \text{(B.20)}$$

$$w_{1l}'(0,t) = w_{1r}'(0,t) = 0 \qquad \text{(B.21)}$$

$$w_{1l}''(H_f,t) = w_{1r}''(H_f,t) = 0 \qquad \text{(B.22)}$$

$$w_{2l}'(H_f,t) = w_{2r}'(H_f,t) = 0 \qquad \text{(B.23)}$$

$$w_{2l}''(2H_f,t) = w_{2r}''(2H_f,t) = 0 \qquad \text{(B.24)}$$

The boundary controller is rewritten as

$$u(t) = 0. \qquad \text{(B.25)}$$

In order to analyze the rewritten system, we use the method of separating variables. Assuming that $w_{2l}(y,t) = P_{2l}(y)Q(t)$, $w_{2r}(y,t) = P_{2r}(y)Q(t)$, $w_{1l}(y,t) = P_{1l}(y)Q(t)$ and $w_{1r}(y,t) = P_{1r}(y)Q(t)$, we obtain the following equations.

$$\frac{EIP_{2l}''''(y) - TP_{2l}''(y)}{\rho P_{2l}(y)} = -\frac{\ddot{Q}(t)}{Q(t)} \qquad \text{(B.26)}$$

$$\frac{EIP_{2r}''''(y) - TP_{2r}''(y)}{\rho P_{2r}(y)} = -\frac{\ddot{Q}(t)}{Q(t)} \qquad \text{(B.27)}$$

$$\frac{EIP_{1l}''''(y) - TP_{1l}''(y)}{\rho P_{1l}(y)} = -\frac{\ddot{Q}(t)}{Q(t)} \qquad \text{(B.28)}$$

$$\frac{EIP_{1r}''''(y) - TP_{1r}''(y)}{\rho P_{1r}(y)} = -\frac{\ddot{Q}(t)}{Q(t)} \qquad \text{(B.29)}$$

$$P_2(2H_f) = P_1(H_f) = 0 \qquad \text{(B.30)}$$

$$P_{1l}(0) = P_{1r}(0) = 0 \qquad \text{(B.31)}$$

$$P_{1l}'(0) = P_{1r}'(0) = 0 \qquad \text{(B.32)}$$

$$P_{1l}''(H_f,t) = P_{1r}''(H_f,t) = 0 \qquad \text{(B.33)}$$

$$P_{2l}'(H_f,t) = P_{2r}'(H_f,t) = 0 \qquad \text{(B.34)}$$

$$P_{2l}''(2H_f,t) = P_{2r}''(2H_f,t) = 0. \qquad \text{(B.35)}$$

Defining $-\frac{\ddot{Q}(t)}{Q(t)} = \varepsilon$ where ε is a constant. At first we analyze $P_{2l}(y)$.

$$P_{2l}''''(y) - \frac{T}{EI}P_{2l}''(y) - \frac{\varepsilon\rho}{EI}P_{2l}(y) = 0 \qquad \text{(B.36)}$$

The characteristic equation is $\lambda^4 - \frac{T}{EI}\lambda^2 - \frac{\varepsilon\rho}{EI} = 0$

1)If $\varepsilon > 0$, the characteristic values are $\lambda_1 = \sqrt{\frac{\frac{T}{EI}+b}{2}}$, $\lambda_2 = -\sqrt{\frac{\frac{T}{EI}+b}{2}}$, $\lambda_3 = \sqrt{\frac{b-\frac{T}{EI}}{2}}i$ and $\lambda_4 = -\sqrt{\frac{b-\frac{T}{EI}}{2}}i$, where $b = \sqrt{\frac{T^2}{EI^2} + \frac{4\varepsilon\rho}{EI}}$. The general solution of (B.36) is

$$\begin{aligned}
P_{2l}(y) =\ & C_3\cos(\sqrt{\frac{\frac{T}{EI}-b}{2}}y) + C_4\sin(\sqrt{\frac{\frac{T}{EI}-b}{2}}y) \\
& +C_1e^{\sqrt{\frac{\frac{T}{EI}+b}{2}}y} + C_2e^{-\sqrt{\frac{\frac{T}{EI}+b}{2}}y} \qquad \text{(B.37)}
\end{aligned}$$

Substituting (B.30)-(B.33), we have

$$\begin{aligned}
P_{2l}(H_f) =\ & C_1e^{\sqrt{\frac{\frac{T}{EI}+b}{2}}H_f} + C_2e^{-\sqrt{\frac{\frac{T}{EI}+b}{2}}H_f} \\
& +C_3\cos(\sqrt{\frac{b-\frac{T}{EI}}{2}}H_f)
\end{aligned}$$

$$+C_4\sin(\sqrt{\frac{b-\frac{T}{EI}}{2}}H_f)=0 \quad \text{(B.38)}$$

$$\begin{aligned}P_{2l}(2H_f) =\ & C_1e^{2\sqrt{\frac{\frac{T}{EI}+b}{2}}H_f}+C_2e^{-2\sqrt{\frac{\frac{T}{EI}+b}{2}}H_f}\\ &+C_3\cos(2\sqrt{\frac{b-\frac{T}{EI}}{2}}H_f)\\ &+C_4\sin(2\sqrt{\frac{b-\frac{T}{EI}}{2}}H_f)=0\end{aligned} \quad \text{(B.39)}$$

$$\begin{aligned}P'_{2l}(H_f) =\ & \sqrt{\frac{\frac{T}{EI}+b}{2}}C_1e^{\sqrt{\frac{\frac{T}{EI}+b}{2}}H_f}\\ &-\sqrt{\frac{\frac{T}{EI}+b}{2}}C_2e^{-\sqrt{\frac{\frac{T}{EI}+b}{2}}H_f}\\ &-\sqrt{\frac{b-\frac{T}{EI}}{2}}C_3\sin(\sqrt{\frac{b-\frac{T}{EI}}{2}}H_f)\\ &+\sqrt{\frac{b-\frac{T}{EI}}{2}}C_4\cos(\sqrt{\frac{b-\frac{T}{EI}}{2}}H_f)=0\end{aligned} \quad \text{(B.40)}$$

$$\begin{aligned}P''_{2l}(2H_f) =\ & \frac{\frac{T}{EI}+b}{2}C_1e^{2\sqrt{\frac{\frac{T}{EI}+b}{2}}H_f}\\ &+\frac{\frac{T}{EI}+b}{2}C_2e^{-2\sqrt{\frac{\frac{T}{EI}+b}{2}}H_f}\\ &-\frac{b-\frac{T}{EI}}{2}C_3\cos(2\sqrt{\frac{b-\frac{T}{EI}}{2}}H_f)\\ &-\frac{b-\frac{T}{EI}}{2}C_4\sin(2\sqrt{\frac{b-\frac{T}{EI}}{2}}H_f)=0\end{aligned} \quad \text{(B.41)}$$

From (B.38)-(B.41), we have $C_1 = C_2 = C_3 = C_4 = 0$, namely, (B.37) is a trivial solution.

2)If $\varepsilon = 0$, the characteristic values are $\lambda_1 = 0$, $\lambda_2 = 0$, $\lambda_3 = \sqrt{\frac{T}{EI}}$ and $\lambda_4 = -\sqrt{\frac{T}{EI}}$. The general solution of (B.36) is

$$P_{2l}(y) = C_1 + C_2y + C_3e^{\sqrt{\frac{T}{EI}}y} + C_4e^{-\sqrt{\frac{T}{EI}}y} \quad \text{(B.42)}$$

Substituting (B.30)-(B.33), we have

$$\begin{aligned}P_{2l}(H_f) =\ & C_1 + C_2H_f + C_3e^{\sqrt{\frac{T}{EI}}H_f}\\ &+C_4e^{-\sqrt{\frac{T}{EI}}H_f}=0\end{aligned} \quad \text{(B.43)}$$

$$\begin{aligned}P_{2l}(H_f) =\ & C_1 + 2C_2H_f + C_3e^{2\sqrt{\frac{T}{EI}}H_f}\\ &+C_4e^{-2\sqrt{\frac{T}{EI}}H_f}=0\end{aligned} \quad \text{(B.44)}$$

$$\begin{aligned}P'_{2l}(H_f) =\ & C_2+\sqrt{\frac{T}{EI}}C_3e^{\sqrt{\frac{T}{EI}}H_f}\\ &-\sqrt{\frac{T}{EI}}C_4e^{-\sqrt{\frac{T}{EI}}H_f}=0\end{aligned} \quad \text{(B.45)}$$

$$P''_{2l}(2H_f) = \frac{TC_3}{EI}e^{2\sqrt{\frac{T}{EI}}H_f}+\frac{TC_4}{EI}e^{-2\sqrt{\frac{T}{EI}}H_f}=0 \quad \text{(B.46)}$$

From (B.43)-(B.46), we have $C_1 = C_2 = C_3 = C_4 = 0$, namely, (B.42) is a trivial solution.

3)If $-\frac{T^2}{4EI\rho} < \varepsilon < 0$, the characteristic values are $\lambda_1 = \sqrt{\frac{\frac{T}{EI}+b}{2}}$, $\lambda_2 = -\sqrt{\frac{\frac{T}{EI}+b}{2}}$, $\lambda_3 = \sqrt{\frac{\frac{T}{EI}-b}{2}}$ and $\lambda_4 = -\sqrt{\frac{\frac{T}{EI}-b}{2}}$, where $b = \sqrt{\frac{T^2}{EI^2}+\frac{4\varepsilon\rho}{EI}}$. The general solution of (B.36) is

$$\begin{aligned}P_l(y) =\ & C_1e^{\sqrt{\frac{\frac{T}{EI}+b}{2}}y}+C_2e^{-\sqrt{\frac{\frac{T}{EI}+b}{2}}y}+C_3e^{\sqrt{\frac{\frac{T}{EI}-b}{2}}y}\\ &+C_4e^{-\sqrt{\frac{\frac{T}{EI}-b}{2}}y}\end{aligned} \quad \text{(B.47)}$$

Substituting (B.30)-(B.33), we have

$$\begin{aligned}P_{2l}(H_f) =\ & C_1e^{\sqrt{\frac{\frac{T}{EI}+b}{2}}H_f}+C_2e^{-\sqrt{\frac{\frac{T}{EI}+b}{2}}H_f}\\ &+C_3e^{\sqrt{\frac{\frac{T}{EI}-b}{2}}H_f}+C_4e^{-\sqrt{\frac{\frac{T}{EI}-b}{2}}H_f}=0\end{aligned} \quad \text{(B.48)}$$

$$\begin{aligned}P_{2l}(2H_f) =\ & C_1e^{2\sqrt{\frac{\frac{T}{EI}+b}{2}}H_f}+C_2e^{-2\sqrt{\frac{\frac{T}{EI}+b}{2}}H_f}\\ &+C_3e^{2\sqrt{\frac{\frac{T}{EI}-b}{2}}H_f}+C_4e^{-2\sqrt{\frac{\frac{T}{EI}-b}{2}}H_f}=0\end{aligned} \quad \text{(B.49)}$$

$$\begin{aligned}P'_{2l}(H_f) =\ & \sqrt{\frac{\frac{T}{EI}+b}{2}}\Big(C_1e^{\sqrt{\frac{\frac{T}{EI}+b}{2}}H_f}-C_2e^{-\sqrt{\frac{\frac{T}{EI}+b}{2}}H_f}\Big)\\ &+\sqrt{\frac{\frac{T}{EI}-b}{2}}C_3e^{\sqrt{\frac{\frac{T}{EI}-b}{2}}H_f}\\ &-\sqrt{\frac{\frac{T}{EI}-b}{2}}C_4e^{-\sqrt{\frac{\frac{T}{EI}-b}{2}}H_f}=0\end{aligned} \quad \text{(B.50)}$$

$$\begin{aligned}P''_{2l}(2H_f) =\ & \frac{\frac{T}{EI}+b}{2}\Big(C_1e^{2\sqrt{\frac{\frac{T}{EI}+b}{2}}H_f}+C_2e^{-2\sqrt{\frac{\frac{T}{EI}+b}{2}}H_f}\Big)\\ &+\frac{\frac{T}{EI}-b}{2}C_3e^{2\sqrt{\frac{\frac{T}{EI}-b}{2}}H_f}\\ &+\frac{\frac{T}{EI}-b}{2}C_4e^{-2\sqrt{\frac{\frac{T}{EI}-b}{2}}H_f}=0\end{aligned} \quad \text{(B.51)}$$

From (B.48)-(B.51), we have $C_1 = C_2 = C_3 = C_4 = 0$, namely, (B.47) is a trivial solution.

4)If $\varepsilon = -\frac{T^2}{4EI\rho}$, the characteristic values are $\lambda_1 = \lambda_2 = \sqrt{\frac{T}{2EI}}$ and $\lambda_3 = \lambda_4 = -\sqrt{\frac{T}{2EI}}$. The general solution of (B.36) is

$$P_{2l}(y) = (C_1 + C_2y)e^{\sqrt{\frac{T}{2EI}}y} + (C_3 + C_4y)e^{-\sqrt{\frac{T}{2EI}}y} \quad \text{(B.52)}$$

Substituting (B.30)-(B.33), we have

$$\begin{aligned}P_{2l}(H_f) =\ & (C_1 + C_2H_f)e^{\sqrt{\frac{T}{2EI}}H_f}\\ &+(C_3 + C_4H_f)e^{-\sqrt{\frac{T}{2EI}}H_f}=0\end{aligned} \quad \text{(B.53)}$$

$$\begin{aligned}P_{2l}(2H_f) =\ & (C_1 + 2C_2H_f)e^{2\sqrt{\frac{T}{2EI}}H_f}\\ &+(C_3 + 2C_4H_f)e^{-2\sqrt{\frac{T}{2EI}}H_f}=0\end{aligned} \quad \text{(B.54)}$$

$$
\begin{aligned}
P_{2l}'(H_f) &= C_2 e^{\sqrt{\frac{T}{2EI}}H_f} + C_4 e^{-\sqrt{\frac{T}{2EI}}H_f} \\
&\quad +(C_1 + C_2 H_f)\sqrt{\frac{T}{2EI}} e^{\sqrt{\frac{T}{2EI}}H_f} \\
&\quad -(C_3 + C_4 H_f)\sqrt{\frac{T}{2EI}} e^{-\sqrt{\frac{T}{2EI}}H_f} = 0 \text{(B.55)} \\
P_{2l}''(2H_f) &= 2\sqrt{\frac{T}{2EI}}\Big(C_2 e^{2\sqrt{\frac{T}{2EI}}H_f} - C_4 e^{-2\sqrt{\frac{T}{2EI}}H_f}\Big) \\
&\quad +(C_1 + 2C_2 H_f)\frac{T}{2EI} e^{2\sqrt{\frac{T}{2EI}}H_f} \\
&\quad +(C_3 + 2C_4 H_f)\frac{T}{2EI} e^{-2\sqrt{\frac{T}{2EI}}H_f} = 0 \text{ (B.56)}
\end{aligned}
$$

From (B.53)-(B.56), we have $C_1 = C_2 = C_3 = C_4 = 0$, namely, (B.52) is a trivial solution.

5)If $\varepsilon < -\frac{T^2}{4EI\rho}$, the characteristic values are $\lambda_1 = \varphi + \psi i$, $\lambda_2 = \varphi - \psi i$, $\lambda_3 = -\varphi + \psi i$ and $\lambda_4 = -\varphi - \psi i$, where $\varphi = \frac{\sqrt{\frac{T}{EI}+2\sqrt{-\frac{\varepsilon\rho}{EI}}}}{2}$ and $\psi = \frac{\sqrt{-\frac{T}{EI}+2\sqrt{-\frac{\varepsilon\rho}{EI}}}}{2}$. The general solution of (B.36) is

$$
\begin{aligned}
P_{2l}(y) &= e^{\varphi y}(C_1\cos(\psi y) + C_2\sin(\psi y)) \\
&\quad +e^{-\varphi y}(C_3\cos(\psi y) + C_4\sin(\psi y)) \quad \text{(B.57)}
\end{aligned}
$$

Substituting (B.30)-(B.33), we can find that the solution of (B.36) is $P_{2l}(y) = 0$.

Then because the differential equation of $P_{2r}(y)$ and $w_{2l}(y,t) = 0$, $P_{2r}''''(y) - \frac{\varepsilon\rho}{EI}P_{2r}(y) = 0$, and the boundary conditions of $P_{2r}(y)$ are similar with $P_{2l}(y)$, we can obtain $P_{2r}(y) = 0$ and $w_{2r}(y,t) = 0$. Similarly, we have $w_{1l}(y,t) = w_{1r}(y,t) = 0$. Combining with (B.8), we can obtain $\dot{V}(t) = 0$ if and only if states are zero.

C. Proof of Property 3

Proof: Differentiating the Lyapunov function candidate (29)

$$
\begin{aligned}
\dot{E}(t) &= \dot{V}(t) + \chi_1\dot{\widetilde{EI}}(t)\widetilde{EI}(t) + \chi_2\dot{\tilde{T}}(t)\tilde{T}(t) \\
&\quad +\chi_3\dot{\tilde{M}}_f(t)\tilde{M}_f(t) \quad \text{(C.1)}
\end{aligned}
$$

Substituting the adaptive boundary controller into the derivation of (20), we have

$$
\begin{aligned}
\dot{V}_b(t) &= \Big(M_c + \frac{M_c + J_c}{J_c}M_f\Big)\mu(t)\dot{\mu}(t) \\
&= -k[\mu(t)]^2 + \mu(t)\{-\frac{M_c + J_c}{J_c}\widehat{EI}(t)[w_{2r}'''(2H_f,t) \\
&\quad +w_{2l}'''(2H_f,t)] + \frac{M_c + J_c}{J_c}\hat{T}(t)[w_{2l}'(2H_f,t) \\
&\quad +w_{2r}'(2H_f,t)] + \gamma_1\Big(\frac{M_c + J_c}{J_c}\hat{M}_f(t) + M_c\Big) \\
&\quad \times[\dot{w}_{2l}'''(2H_f,t) + \dot{w}_{2r}'''(2H_f,t)] - \gamma_2\Big(\frac{M_c + J_c}{J_c}\hat{M}_f(t) \\
&\quad +M_c\Big)[\dot{w}_{2l}'(2H_f,t) + \dot{w}_{2r}'(2H_f,t)] + \frac{M_c + J_c}{J_c}EI \\
&\quad \times[w_{2l}'''(2H_f,t) + w_{2r}'''(2H_f,t)] - \frac{M_c + J_c}{J_c}T \\
&\quad \times[w_{2l}'(2H_f,t) + w_{2r}'(2H_f,t)] - \Big(\frac{(M_c + J_c)M_f}{J_c} \\
&\quad +M_c\Big)\gamma_1[\dot{w}_{2l}'''(2H_f,t) + \dot{w}_{2r}'''(2H_f,t)] + \Big(M_c \\
&\quad +\frac{(M_c + J_c)M_f}{J_c}\Big)\gamma_2[\dot{w}_{2l}'(2H_f,t) + \dot{w}_{2r}'(2H_f,t)]\} \\
&= -k[\mu(t)]^2 + \mu(t)\{\frac{M_c + J_c}{J_c}\widetilde{EI}(t)[w_{2r}'''(2H_f,t) \\
&\quad +w_{2l}'''(2H_f,t)] - \frac{M_c + J_c}{J_c}\tilde{T}(t)[w_{2l}'(2H_f,t) \\
&\quad +w_{2r}'(2H_f,t)] - \gamma_1\frac{M_c + J_c}{J_c}\tilde{M}_f(t)[\dot{w}_{2l}'''(2H_f,t) \\
&\quad +\dot{w}_{2r}'''(2H_f,t)] + \gamma_2\frac{M_c + J_c}{J_c}\tilde{M}_f(t)[\dot{w}_{2l}'(2H_f,t) \\
&\quad +\dot{w}_{2r}'(2H_f,t)]\} \quad \text{(C.2)}
\end{aligned}
$$

Using adaptation laws, we obtain

$$
\begin{aligned}
\dot{E}(t) &= \mu(t)\{\frac{M_c + J_c}{J_c}\widetilde{EI}(t)[w_{2r}'''(2H_f,t) + w_{2l}'''(2H_f,t)] \\
&\quad -\frac{M_c + J_c}{J_c}\tilde{T}(t)[w_{2l}'(2H_f,t) + w_{2r}'(2H_f,t)] \\
&\quad -\gamma_1\frac{M_c + J_c}{J_c}\tilde{M}_f(t)[\dot{w}_{2l}'''(2H_f,t) + \dot{w}_{2r}'''(2H_f,t)] \\
&\quad +\gamma_2\frac{M_c + J_c}{J_c}\tilde{M}_f(t)[\dot{w}_{2l}'(2H_f,t) + \dot{w}_{2r}'(2H_f,t)]\} \\
&\quad +\dot{V}(t) + \chi_1\dot{\widetilde{EI}}(t)\widetilde{EI}(t) + \chi_2\dot{\tilde{T}}(t)\tilde{T}(t) \\
&\quad +\chi_3\dot{\tilde{M}}_f(t)\tilde{M}_f(t) \\
&= \dot{V}(t) - \{\chi_1\dot{\widetilde{EI}}(t) - \mu(t)\frac{M_c + J_c}{J_c}[w_{2r}'''(2H_f,t) \\
&\quad +w_{2l}'''(2H_f,t)]\}\widetilde{EI}(t) - \{\chi_2\dot{\tilde{T}}(t) + \mu(t)\frac{M_c + J_c}{J_c} \\
&\quad \times[w_{2l}'(2H_f,t) + w_{2r}'(2H_f,t)]\}\tilde{T}(t) - \{\chi_3\dot{\tilde{M}}_f(t) \\
&\quad +\mu(t)\gamma_1\frac{M_c + J_c}{J_c}[\dot{w}_{2l}'''(2H_f,t) + \dot{w}_{2r}'''(2H_f,t)] \\
&\quad -\mu(t)\gamma_2\frac{M_c + J_c}{J_c}[\dot{w}_{2l}'(2H_f,t) \\
&\quad +\dot{w}_{2r}'(2H_f,t)]\}\tilde{M}_f(t) \\
&= \dot{V}(t) \quad \text{(C.3)}
\end{aligned}
$$

Referencing the derivation in Appendix B, we can obtain $\dot{E}(t) = 0$ if and only if states are zero.

Jiali Feng received the B. Eng. degree and M.E. degree in School of Automation and Electrical Engineering, University of Science and Technology Beijing (USTB), Beijing, China in 2017 and 2020. Her current research interests include distributed parameter system and vibration control.

Zhijie Liu (S'17-M'19) received B.Sc. degree from China University of Mining and Technology Beijing, Beijing, China in 2014, and the Ph.D degree from Beihang University, Beijing, China in 2019. In 2017, he was a Research Assistant with the Department of Electrical Engineering, University of Notre Dame, for twelve months. He is currently an Associate Professor with the School of Automation and Electrical Engineering, University of Science and Technology Beijing, Beijing, China.

He is a recipient of the IEEE SMC Beijing Captital Region Chapter Young Author Prize Award in 2019. He is the member of IEEE SMC Technical Committee on Autonomous Bionic Robotic Aircraft.

His research interests include adaptive control, modeling and vibration control for flexible structures, and distributed parameter system.

Xiuyu He (S'15-M'19) received the B.Eng. degree in automation from Hubei University of Technology, China in 2012, received the M.E. degree in Control Science and Engineering, University of Electronic Science and Technology of China (UESTC), Chengdu, China in 2016, and received the Ph.D. degree in Control Science and Engineering, University of Science and Technology Beijing (USTB), Beijing, China in 2020. He is currently working as an associate professor in School of Automation and Electrical Engineering, University of Science and Technology Beijing, Beijing, China. His current research interests include distributed parameter system, marine cybernetics and robotics.

QIANG FU received the B.S. degree in thermal energy and power engineering from Beijing Jiaotong University, Beijing, China, in 2009, and the Ph.D. degree in control science and engineering from Beihang University (formerly Beijing University of Aeronautics and Astronautics), Beijing, China, in 2016. ? He is currently an associate professor in the School of Automation and Electrical Engineering, University of Science and Technology Beijing. His main research interests include vision-based navigation and robotic visual servoing.

Guang Li (M'09) received his PhD degree in Electrical and Electronics Engineering, specialized in control systems, from the University of Manchester, in 2007. He is currently a Senior Lecturer in dynamics modelling and control in Queen Mary University of London, UK. His current research interests include constrained optimal control, model predictive control, adaptive robust control and control applications including renewable energies and energy storage, etc.